

Connection between Optical Frequency Combs and Microwave Frequency Combs Produced by Active-Mode-Locked Lasers Subject to Timing Jitter

D.S. Citrin^{1,2,*}

¹*School of Electrical and Computer Engineering, Georgia Institute of Technology, Atlanta, Georgia 30332-0250, USA*

²*Georgia Tech-CNRS IRL-2958, Georgia Tech Lorraine, 2 Rue Marconi, 57070 Metz, France*

(Received 9 March 2021; revised 26 April 2021; accepted 30 April 2021; published 2 July 2021)

Optical frequency combs (OFCs) and microwave frequency combs (MFCs) are of intense interest in fields ranging from metrology to multifrequency light sources. MFCs in particular have attracted interest for applications in microwave photonics. Timing jitter is a key limiting factor of the quality of OFCs and MFCs, and despite the central importance of timing jitter, a clear generic account of its effect on OFCs and MFCs that provides a connection between the two is lacking. We consider the power spectral density (PSD) of the OFCs and MFCs produced by active and hybrid active-passive mode-locked lasers in which the active mode locking is effected by a high-spectral-purity oscillator, but with timing noise originating in both the active locking and the mode-locked oscillators. Based on an analytically tractable theoretical treatment, we account quantitatively for the characteristic comb line shape consisting of a narrow central peak lying atop a broad pedestal. The theory provides a quantitative comparison between characteristic OFC and MFC line shapes and identifies the origin of the difference.

DOI: [10.1103/PhysRevApplied.16.014004](https://doi.org/10.1103/PhysRevApplied.16.014004)

I. INTRODUCTION

Mode-locked lasers (MLLs) [1] are a central technology at the foundation of ultrafast optics. Self-MLLs [2] do not require any external modulation to produce trains of short optical pulses; however, for some laser types, self-mode locking is difficult to achieve or, if it can be achieved, may be plagued by unacceptably high levels of jitter in the pulse timing. Active mode locking [3] requires external modulation and although the shortest pulses and highest repetition rates may not be accessible through active mode locking, it has proven to be an important tool to stabilize locking and has also proven instrumental in reducing the effects of noise in the ultimate output of the MLL. Hybrid active-passive mode locking [4] is also employed, particularly in semiconductor lasers [5].

Large classes of mode-locking mechanisms—additive-pulse mode locking, saturable-absorber mode locking with self-phase modulation and group-velocity dispersion, Kerr-lens mode locking, and various types of hybrid mode locking—are described by similar models based on the Haus master equation [6–8]. Depending upon the effects included, the Haus master equation describes the temporal optical pulse shapes produced, the mode locking itself, and the effects of various types of noise. It has been observed and described theoretically that in hybrid MMLs,

the spectral widths of optical-frequency-comb (OFC) lines are much narrower than what is attained omitting the active modulation and that the narrow central lines lie atop a broad pedestal or continuum [9–19]. This effect is clearly accounted for in the theory of Ref. [9], where it is found that it is due to the nature of the autocorrelation function (acf) of the timing jitter. In the case of no active mode locking, the timing jitter can wander without bound and is described by a Wiener process (one-dimensional diffusion) [20], whereas the active locking imposes a restoring force on the timing jitter.

Apart from the direct use of the ultrafast optical pulse produced by MLLs, trains of highly stable optical pulses at a well-defined repetition rate f_{rep} give rise in the spectral domain to an optical frequency comb (OFC) with a spectrum consisting of a set of narrow lines separated by f_{rep} . OFCs have numerous metrological and other applications that have been under intense exploration [21–23]. In order to form an OFC, there must be some degree of mutual coherence between the electric fields $E(t)$ of the pulses. MFCs [24,25] are of increasing interest for applications in microwave photonics [26,27]. We shall see that less stringent requirements for comb formation apply to microwave frequency combs (MFC), which are formed by the train of the optical intensity $I(t) = |E(t)|^2$. In other words, MFCs can be generated under circumstances where OFC quality may be poor. Understandably, there has been intense interest in the shape of comb lines—for

* david.citrin@ece.gatech.edu

both OFCs and MFCs—and the effects of noise of various types [28–31].

As pointed out above, while self-MLLs provide for the shortest pulses and the broadest OFCs, they may suffer from poor mode locking and significant timing jitter. In addition, there may be a lack of control of absolute timing of the pulses; in the absence of further intervention, timing jitter can lead to an eventual wandering of the absolute timing of the pulses. Active means to stabilize timing in OFCs can circumvent such problems, though often at the cost of producing longer pulses and thus combs of reduced bandwidth. In Ref. [32], an electro-optic modulator has been used to modulate cw laser light injected into an optical resonator to produce an OFC and bandwidths on the order of terahertz have been demonstrated [33]. Active mode locking has also been employed for OFC generation [34–37]. In Refs. [24,25], active mode locking has been used to specifically generate MFCs. Our aim in this study is to ascertain the effect of timing jitter on OFCs and MFCs generated by active MLLs and hybrid MLLs. While considerable work has focused on important figures of merit associated with OFCs and MFCs, such as bandwidth, flatness, and comb line shape, the relationship between line shape and noise in OFCs and MFCs *and their relationship* is only sparsely explored.

In previous work, we have studied the effect of carrier-envelope (CE) phase fluctuations in CE-stabilized OFCs on the power spectral density (PSD) [38]. We have found, in a CE-phase-noise model, that the comb line shape is Gaussian and the resulting OFC is periodic in the frequency domain, overlain by an envelope given by the power spectrum $|\tilde{\mathcal{A}}(\nu)|^2$ of the optical pulse envelope $A(t)$, where $\tilde{\mathcal{A}}(\nu)$ is the Fourier transform of $\mathcal{A}(t)$ (see below for precise definitions). In Ref. [39], the effects of phase noise on the PSD of the optical output of an injection-locked optoelectronic oscillator have been treated. The PSD has been shown to consist of a narrow central portion of the line on top of a broader pedestal. While this type of effect has been noted for a range of locked oscillators, the heuristic understanding of the effect of a spectrally pure locking oscillator on the output of the locking oscillator is clear, and the difference between a self-sustaining [20] and a locked oscillator [4] is understood, there is a surprising lack of rigorous mathematical underpinning of this effect. The results of Ref. [39] are particularly pertinent to our present study, as the output of the active MLL consists of many sinusoidally varying modes, each with phase noise connected via the timing jitter.

Our aim in the present study therefore is to focus on timing jitter, i.e., the deviation of the occurrences of the pulses from their ideal periodic temporal location and the effect on the resulting OFCs and MFCs. We distinguish three relevant PSDs. The PSD of the OFC is denoted $S_E(\nu)$, where ν is the frequency and $E = E(t)$ indicates the electric field of the optical pulse train. The PSD of

the MFC is denoted $S_I(\nu)$, where $I = I(t)$ indicates the intensity of the optical pulse train. $S_f(\nu)$ is the Wiener-Kinchine PSD [40–42] of a train of otherwise temporally equispaced Dirac δ functions but subject to timing jitter. For convenience, we consider the two-sided PSD, though readers more interested in the one-sided PSD more closely related to certain standards [43] can easily adapt our approach. In the absence of timing jitter, $S_f(\nu)$ is a Dirac comb, i.e., a periodic sequence of Dirac δ functions separated by f_{rep} , modulated overall by the appropriate power spectrum of a single pulse. $S_E(\nu)$ and $S_I(\nu)$ are then obtained from $S_f(\nu)$ by multiplying by the relevant single-pulse power spectrum.

In summary, our main findings are as follows. (1) Following the approach of Refs. [4,10], we obtain an expression for the PSDs of the OFC and MFC based on a small number of generic empirical parameters. The explicit calculation is given making clear the role of the relevant stochastic processes relating timing jitter to the PSDs. The approach is heuristic and can be applied to understand measured comb line spectra, which is especially useful in the absence of knowledge of the plethora of parameters that enter into the theory of Ref. [10]. Although we treat a single fundamental noise source underlying the timing jitter, in our treatment the contributions can be taken to be additive (if, indeed, that is an adequate approach). It should be noted that our approach does not account for stabilization approaches involving time-delay feedback or approaches that might lead to a nonharmonic timing-jitter restoring force. (2) Our treatment makes clear the key step of replacing the Fokker-Planck equation following from the Adler equation with an additional white-noise term by an Ornstein-Uhlenbeck (OU) process to obtain an exact result for the expectation of the time-jitter acf. (3) For the same MLL parameters, the MFC is dominated by comb lines with a narrow line center and a weak and broader pedestal, while the OFC has broader and weaker line centers and broad and stronger pedestals (sometimes called the continuum in the literature). The MFC lines tend to be narrower than OFC lines for the same MLL.

Thus we begin with an otherwise periodic ideal impulse train denoted by $\Pi(t) = \sum_{k=-\infty}^{\infty} \delta(t - k)$, subject to errors in the times k when the impulses occur. We choose the repetition rate f_{rep} to be unity, realizing that we can scale the results to arbitrary f_{rep} . (Alternatively, we work in time units of f_{rep}^{-1} and frequency units of f_{rep} .) We include timing jitter by including a random variable (stochastic delay [44]) $\xi(t)$, so that the pulse train considered is $f(t) = \Pi[t - \xi(t)]$, where $\xi(t)$ has zero mean and the acf $\langle \xi(t)\xi(t - \tau) \rangle$ (structure factor) of $\xi(t)$ depends only on τ . While $\xi(t)$ only manifests itself at discrete times, i.e., provided that $\xi(t)$ varies slowly on the time scale f_{rep}^{-1} , $\xi(k)$ is the timing fluctuation of the k th pulse. Furthermore, we assume that $\xi(t)$, stabilized by active mode locking, obeys an OU process [45]. Emphatically, we do not account for

physical complications such as departures from stationarity or the presence of multiple mechanisms underlying the timing jitter; nor do we account for complications arising from the measurement, such as finite duration of measurements or noise that might be present in the measuring instrument. Other noise types, such as amplitude noise, CE-phase noise, and absolute phase noise, are not considered here. Our focus is on a tractable approach that nonetheless may provide insight or improved results for the spectral properties of signals with timing jitter.

Finally, $S_f(\nu)$ is related to $S_E(\nu)$ and to $S_I(\nu)$ as discussed below. The optical field $E(t)$ is composed of a train of optical pulses with the single-pulse electric field $\mathcal{A}(t)$. To obtain $E(t)$, we convolve $f(t)$ with the field of the optical pulse $\mathcal{A}(t) = A(t) \cos(2\pi\nu_0 t)$, where $A(t)$ is the pulse envelope and ν_0 is the optical carrier frequency,

We present the model in Sec. II. Section III discusses general issues pertaining to jitter statistics. In Sec. IV, we consider the presence of timing jitter in the oscillator providing the active mode locking and in Sec. V we present results relevant to OFCs and MFCs. Section VI contains our conclusions.

II. MODEL

In this section, we outline the basic approach to obtaining the PSDs $S_I(\nu)$ and $S_E(\nu)$. We only account for timing jitter, although in reality other types of noise, likely correlated with the timing jitter, will also be present. As we argue, the key quantity underlying $S_I(\nu)$ and $S_E(\nu)$ is the PSD $S_f(\nu)$ of the impulse train $f(t)$ subject to timing jitter and thus we focus on $S_f(\nu)$. We shall see that (as is well known—for example, from Ref. [44]) that $S_f(\nu)$ is the Fourier transform of the acf of $f(t)$. Our notation for averages over statistical quantities will be more familiar to physicists, indicating such averages by angle brackets. For example, we will indicate the acf of $f(t)$ by $\langle f(\tau)f(0) \rangle$ in favor of the notation $R_f(\tau)$ —the notational convention more familiar to engineers.

We consider an optical pulse train produced by an active MLL, the optical field given by

$$\begin{aligned} E(t) &= \mathcal{A}(t) * f(t), \\ I(t) &= |\mathcal{A}(t)|^2 * f(t) = |A(t)|^2 * f(t), \end{aligned} \quad (1)$$

where $f(t) = \text{III}[t - \xi(t)]$, $\mathcal{A}(t)$ is the electric field of an individual pulse, incorporating both the carrier wave $\cos(2\pi i\nu_0 t)$ and the envelope $A(t)$ as defined above, $*$ is the convolution, $\text{III}(t) = \sum_{k=-\infty}^{\infty} \delta(t - k)$, and $\xi(t)$ is a zero-mean stationary random signal with only second-order correlations, characterizing the timing jitter [46]. Thus, $f(t)$ is an almost-periodic pulse train, i.e., a pulse train with timing jitter. We assume that $\xi(t)$ varies slowly on the time scale of the repetition rate f_{rep} (here assumed, for simplicity, to be 1) (i.e., the correlation time $\tilde{\tau}$ of

$\xi(t)$ satisfies $\tilde{\tau} \gg f_{\text{rep}}^{-1}$ so that the effect of $\xi(t)$ is on the timing jitter and does not significantly affect the pulse-to-pulse coherence). We do not include amplitude noise or absolute-phase noise and we assume that $\xi(t)$ has zero mean $\langle \xi(t) \rangle = 0$, where $\langle a(t) \rangle$ for time-dependent function $a(t)$ denotes the time average of the quantity in the brackets, viz.,

$$\langle a(t) \rangle = \lim_{T \rightarrow \infty} \frac{1}{T} \int_{-T/2}^{T/2} dt a(t).$$

We assume that the ergodic hypothesis holds, whereby we may replace the time average by the average over realizations of $\xi(t)$. The only nonzero correlation function is assumed to be $\langle \xi(t_1)\xi(t_2) \rangle$, which is a function solely of $\tau = t_1 - t_2$.

Our focus will be on the PSD $S_f(\nu)$ of the pulse train $f(t)$ subject to timing jitter, as the overall OFC PSD $S_E(\nu)$ is simply given by the product of $S_f(\nu)$ and the power spectrum $|\bar{\mathcal{A}}(\nu)|^2$ (see the definition of the Fourier transform below) of $\mathcal{A}(t)$ as will be restored later in the treatment. Similarly, $S_E(\nu)$ and $S_I(\nu)$ are given by

$$S_E(\nu) = |\bar{\mathcal{A}}(\nu)|^2 S_f(\nu), \quad (2)$$

$$S_I(\nu) = |\overline{|A|^2}(\nu)|^2 S_f(\nu). \quad (3)$$

To proceed, we can re-express Eq. (1) using the Fourier-series representation of $\text{III}(t)$ as

$$f(t) = \sum_{k=-\infty}^{\infty} e^{2\pi i k [t - \xi(t)]}. \quad (4)$$

$S_f(\nu)$ is obtained as follows. We first define the windowed signal as

$$f_T(t) = \begin{cases} f(t), & |t| < T/2, \\ 0, & \text{otherwise.} \end{cases} \quad (5)$$

The Wiener-Khinchine spectrum is then [41,42]

$$S_f(\nu) = \lim_{T \rightarrow \infty} \frac{1}{T} \langle |\bar{f}_T(\nu)|^2 \rangle, \quad (6)$$

where, in general, $\bar{y}(\nu)$ is the Fourier transform of $y(t)$,

$$\bar{f}_T(\nu) = \int_{-\infty}^{\infty} dt f_T(t) e^{-2\pi i \nu t} = \int_{-T/2}^{T/2} dt f(t) e^{-2\pi i \nu t}. \quad (7)$$

Assembling the above results gives

$$S_f(\nu) = \lim_{T \rightarrow \infty} \frac{1}{T} \int_{-T/2}^{T/2} dt_1 \int_{-T/2}^{T/2} dt_2 e^{2\pi i \nu (t_1 - t_2)} \langle f(t_1) f(t_2) \rangle. \quad (8)$$

In fact, as is well known, since this correlation function depends only on τ for a stationary random process, it will

be reduced to a single-time Fourier transform. In other words, the PSD $S_f(\nu)$ is just the Fourier transform of the acf $F(\tau) = \langle f(t-\tau)f(t) \rangle$ inasmuch as time averages only depend on $|\tau| = t_1 - t_2$. The correlation function in Eq. (8) is

$$F(\tau) = \sum_{k_1, k_2=-\infty}^{\infty} \langle \delta[t_1 - \xi(t_1) - k_1] \delta[t_2 - \xi(t_2) - k_2] \rangle, \quad (9)$$

i.e., $S_f(\nu) = \bar{F}(\nu)$. If the variance of the timing jitter $\sigma_{\xi}^2 = \langle \xi(0)\xi(0) \rangle \ll f_{\text{rep}}^{-2}$ and varies slowly on the time scale f_{rep}^{-1} , we can approximate the time arguments in $\xi(t_1)$ and $\xi(t_2)$ in the Dirac δ functions by k_1 and k_2 , respectively, to give

$$F(\tau) = \sum_{k_1, k_2=-\infty}^{\infty} \langle \delta[t_1 - \xi(k_1) - k_1] \delta[t_2 - \xi(k_2) - k_2] \rangle, \quad (10)$$

whence

$$\begin{aligned} S_f(\nu) &= \lim_{T \rightarrow \infty} \frac{1}{T} \sum_{k_1, k_2=-\infty}^{\infty} \int_{-T/2}^{T/2} dt_1 \int_{-T/2}^{T/2} dt_2 e^{2\pi i \nu(t_1-t_2)} \langle \delta[t_1 - \xi(k_1) - k_1] \delta[t_2 - \xi(k_2) - k_2] \rangle \\ &= \lim_{T \rightarrow \infty} \frac{1}{T} \sum_{k_1, k_2=-\infty}^{\infty} \langle e^{2\pi i \nu[k_1 + \xi(k_1)]} e^{-2\pi i \nu[k_2 + \xi(k_2)]} \rangle = \sum_{k=-\infty}^{\infty} e^{2\pi i \nu k} \langle e^{-2\pi i \nu \Xi(k_1, k_2)} \rangle, \end{aligned} \quad (11)$$

where we define $k = k_1 - k_2$ and use the fact that averages involving $\Xi(t_1, t_2) = \xi(t_1) - \xi(t_2)$ depend only on $\tau = t_1 - t_2$. That is, $S_f(\nu)$ is the Fourier transform of $\langle f(\tau)f(0) \rangle$. The average within Eq. (11) is the key quantity to evaluate before we can proceed. It is convenient to consider the random variables $\Xi(t_1, t_2)$ rather than $\xi(t)$. Like $\xi(t)$, $\Xi(t_1, t_2)$ has zero mean.

III. STATISTICAL QUANTITIES

In order to evaluate the statistical averages, we need to specify the timing-jitter statistics. We find (see the Appendix) that on physical grounds, for the ideally stabilized MLL, $\xi(t)$ is a Gaussian random variable with exponential time correlations. Departures from ideal locking are discussed in the following section.

Before we obtain the key statistical quantities, we point out that averaged quantities above can be evaluated in terms of the structure factor $\sigma_{\Xi}^2(\tau) = \langle \Xi^2(\tau, 0) \rangle$. In turn, $\sigma_{\Xi}^2(\tau)$ can be written in terms of $\sigma_{\xi}^2(\tau) = \langle \xi(\tau)\xi(0) \rangle$. By definition,

$$\begin{aligned} \sigma_{\Xi}^2(\tau) &= \langle \Xi^2(\tau, 0) \rangle = \langle [\xi(\tau) - \xi(0)]^2 \rangle \\ &= 2[\langle \xi^2(0) \rangle - \langle \xi(\tau)\xi(0) \rangle] \\ &= 2[\sigma_{\xi}^2 - \sigma_{\xi}^2(\tau)], \end{aligned} \quad (12)$$

where $\sigma_{\xi}^2 = \sigma_{\xi}^2(0)$ is the variance of $\xi(t)$. We also see that $\sigma_{\xi}^2(\tau) = \sigma_{\xi}^2 - \frac{1}{2}\sigma_{\Xi}^2(\tau)$. The next step is to obtain the statistical distribution obeyed by $\xi(t)$.

Timing noise in hybrid MLLs is discussed in Ref. [4]; the results should also broadly apply for active mode locking as well. In that work, an Adler equation [47] [Eq.

(4)–(7) of Ref. [4] is obtained for the timing noise. Our approach in a similar vein is discussed in detail in Refs. [38,39] and in the Appendix. We add a primary white-noise source to the Adler equation, giving a Langevin equation for in our case $\xi(t)$. In the low-noise limit, we approximate the nonlinear force term in this equation by Hooke's law. The Langevin equation is then converted to a Fokker-Planck equation, which is known to describe an OU process (one-dimensional diffusion in a harmonic potential) [48].

At this stage, we summarize those results that are relevant to our study [48]. The probability distribution function (PDF) of $\xi(t)$ is

$$g_{\sigma_{\xi}}(\xi) = (2\pi\sigma_{\xi}^2)^{-1/2} e^{-\xi^2/(2\sigma_{\xi}^2)} \quad (13)$$

and the acf is

$$\sigma_{\xi}^2(\tau) = \langle \xi(\tau)\xi(0) \rangle = \sigma_{\xi}^2 e^{-2|\tau|/\tilde{\tau}}. \quad (14)$$

Though σ_{ξ}^2 and $\tilde{\tau}$ can be related to thermodynamic quantities (see the Appendix), we parametrize our results in terms of empirical quantities σ_{ξ}^2 and $\tilde{\tau}$ themselves. To proceed with $S_f(\omega)$ in Eq. (11), we need the characteristic function

$$\langle \exp[-2\pi i \nu \Xi(\tau, 0)] \rangle = \int_{-\infty}^{\infty} d\Xi g_{\sigma_{\Xi}}(\Xi) e^{-2\pi i \nu \Xi}. \quad (15)$$

[Without loss of generality, we will carry out the integrations over Ξ from $-\infty$ to ∞ and normalize $g_{\sigma_{\Xi}}(\Xi)$

accordingly, as $g_{\sigma_\Xi}(\Xi)$ must be an even function.] We have

$$g_{\sigma_\Xi}(\Xi) = \frac{1}{\sqrt{2\pi\sigma_\Xi^2(\tau)}} \exp\left[-\frac{\Xi^2}{2\sigma_\Xi^2(\tau)}\right]. \quad (16)$$

This is the PDF of Ξ , which in view of the above is closely related to the PDF $g_{\sigma_\xi}(\xi)$ of ξ . Then, from Eq. (15),

$$\langle \exp[-2\pi i v \Xi(\tau, 0)] \rangle = \exp[-2\pi^2 v^2 \sigma_\Xi^2(\tau)]. \quad (17)$$

Consequently, we obtain, from Eq. (11),

$$S_f(v) = \sum_{k=-\infty}^{\infty} e^{-2\pi^2 v^2 \sigma_\Xi^2(k)} e^{2\pi i v k}. \quad (18)$$

Note that due to the fact only the that temporal averages of the fluctuations at times τ close to $k = k_1 - k_2$ contribute to the averaged quantities, cf. Eq. (10), k serves in the role of τ . Equation (18) is almost of the form of a Fourier series; however, the v dependence of the factor $\exp\{\dots\}$ in the summand prevents this. In the absence of this factor, the OFC would be a Dirac comb.

We thus obtain, from Eq. (18),

$$S_f(v) = \sum_{k=-\infty}^{\infty} \exp\left[-4\pi^2 v^2 \sigma_\xi^2 \left(1 - e^{-2|k|/\tilde{\tau}}\right)\right] e^{2\pi i v k}. \quad (19)$$

Equation (19) diverges when $v = n f_{\text{rep}}$ with n an integer and thus we have to remove the divergent part from the summation [49]. We write

$$\begin{aligned} S_f(v) &= e^{-4\pi^2 v^2 \sigma_\xi^2} \sum_{k=-\infty}^{\infty} \left[1 + \left(e^{4\pi^2 v^2 \sigma_\xi^2 e^{-2|k|/\tilde{\tau}}} - 1 \right) \right] e^{2\pi i v k} \\ &= e^{-4\pi^2 v^2 \sigma_\xi^2} \text{III}(v) + e^{-4\pi^2 v^2 \sigma_\xi^2} \sum_{k=-\infty}^{\infty} \left(e^{4\pi^2 v^2 \sigma_\xi^2 e^{-2|k|/\tilde{\tau}}} - 1 \right) e^{2\pi i v k}. \end{aligned} \quad (20)$$

We see that $S_f(v)$ consists of two types of terms: a Dirac comb modulated in frequency by a Gaussian falling off with v and a term that we shall later see is associated with a pedestal for the peaks centered at the comb frequencies. Note that at $v = 0$, we only have the δ -function peak arising from $e^{-4\pi^2 v^2 \sigma_\xi^2} \text{III}(v)$. We shall discuss the trends in Sec. V, where we present results relevant to OFCs and MFCs.

IV. EFFECT OF TIMING JITTER IN THE LOCKING OSCILLATOR

So far, we have assumed an ideal spectrally pure locking oscillator. This has led to the Dirac-comb contribution to $S_f(v)$. While the locking oscillator will be far more spectrally pure than the locked oscillator under self-mode-locking conditions (this is the entire point of the locking oscillator), the locking oscillator itself is subject to timing jitter. The locking oscillator can be considered as a self-sustaining oscillator (in the sense of Ref. [20]) and therefore its timing can wander over time. In this section, we account for timing jitter in the locking oscillator.

We follow the treatment in Ref. [39]. We denote the timing jitter in the locking oscillator as $\vartheta(t)$, which is assumed to be driven by a Wiener process. The overall timing jitter present in the output of the injection-locked laser is $\varphi(t)$, which contains contributions from $\xi(t)$ (the contribution from the locked oscillator) and from $\vartheta(t)$. If the time scale of fluctuations $\vartheta(t)$ is much slower than the time scale of $\xi(t)$, we assume that $\varphi(t) = \vartheta(t) + \xi(t)$. Furthermore, it is reasonable to suppose that $\xi(t)$ and $\vartheta(t)$ are driven by statistically independent random processes. Note that $\langle \varphi(t) \rangle \neq 0$; however, we do assume $\langle \xi(t) \rangle = 0$, where $\xi(t) = \varphi(t) - \vartheta(t)$. In this case, we can factor $\langle e^{-2\pi i v \Phi(t, t')} \rangle$ with $\Phi_{\pm}(t, t') = \varphi(t) - \varphi(t')$ as $\langle e^{-2\pi i v \Phi(t, t')} \rangle = \langle e^{-2\pi i v \Xi(t, t')} \rangle \langle e^{-2\pi i v \Theta(t, t')} \rangle$ with $\Theta(t, t') = \vartheta(t) - \vartheta(t')$. We have $\langle e^{-2\pi i v \Xi(t, 0)} \rangle = \exp[-2\pi^2 v^2 \sigma_\Xi^2(\tau)]$ as above and $\langle e^{-2\pi i v \Theta(t, 0)} \rangle = \exp[-4\pi^2 v^2 \Lambda_0 \tau]$, where $2\pi f_{\text{rep}} \sqrt{\Lambda_0}$ is the characteristic rate for the standard deviation of the phase error resulting from $\vartheta(\tau)$ to wander per repetition from its initial value $\vartheta(0)$ [20].

Corresponding to Eq. (20), we have

$$S_f(v) = e^{-4\pi^2 v^2 \sigma_\xi^2} \sum_{k=-\infty}^{\infty} e^{-4\pi^2 v^2 \Lambda_0 |k|} \exp\left(4\pi^2 v^2 \sigma_\xi^2 e^{-2|k|/\tilde{\tau}}\right) e^{2\pi i v k}. \quad (21)$$

We can then write $S_f(v) = S_f^{(0)}(v) + S_f^{(1)}(v)$ with

$$\begin{aligned} S_f^{(0)}(v) &= e^{-4\pi^2 v^2 \sigma_\xi^2} \sum_{k=-\infty}^{\infty} e^{-4\pi^2 v^2 \Lambda_0 |k|} e^{2\pi i v k} \\ &= e^{-4\pi^2 v^2 \sigma_\xi^2} \frac{1 - e^{-8\pi^2 v^2 \Lambda_0}}{1 + e^{-8\pi^2 v^2 \Lambda_0} - 2e^{-4\pi^2 v^2 \Lambda_0} \cos 2\pi v}, \end{aligned} \quad (22)$$

$$\begin{aligned}
S_f^{(1)}(\nu) &= e^{-4\pi^2\nu^2\sigma_\xi^2} \sum_{k=-\infty}^{\infty} \\
&\left[\exp\left(4\pi^2\nu^2\sigma_\xi^2 e^{-2|k|/\tilde{\tau}}\right) - 1 \right] e^{-4\pi^2\nu^2\Lambda_0|k|} e^{2\pi i\nu k} \\
&= e^{-4\pi^2\nu^2\sigma_\xi^2} \sum_{l=1}^{\infty} \frac{(4\pi^2\nu^2\sigma_\xi^2)^l}{l!} \\
&\times \frac{1 - e^{-8\pi^2\nu^2\Lambda_l}}{1 + e^{-8\pi^2\nu^2\Lambda_l} - 2e^{-4\pi^2\nu^2\Lambda_l} \cos 2\pi\nu}, \quad (23)
\end{aligned}$$

where $4\pi^2\nu^2\Lambda_l = 4\pi^2\nu^2\Lambda_0 + 2l/\tilde{\tau}$. This is essentially the same as Eq. (112) of Ref. [10]. Note that $S_f^{(0)}(\nu)$ produces the Dirac comb in Eq. (20) in the $\Lambda_0 \rightarrow 0$ limit. The comb line shape consists of a central narrow peak of width $2\pi n f_{\text{rep}} \Lambda_0$ lying on top of a pedestal given by a sum of Lorentzians each depending on the comb-line order n centered at $\nu = n f_{\text{rep}}$. For low orders n , $S_f^{(0)}(\nu)$ dominates but plays a smaller role as n increases, while $S_f^{(1)}(\nu)$ dominates for large n .

V. OPTICAL FREQUENCY COMBS AND MICROWAVE FREQUENCY COMBS

In this section, we use the preceding results to understand the PSD $S_f(\nu)$ and hence $S_E(\nu)$ and $S_I(\nu)$ of the OFC and MFC. We focus on $S_f(\nu)$, as $S_E(\nu)$ and $S_I(\nu)$ rely directly on this quantity. The key point is that MFCs rely on low comb orders, while OFCs rely on intermediate comb orders. We choose parameter values for σ_ξ and $\tilde{\tau}$ to illustrate the effects rather than to model any specific MLL. The key parameters to consider are Λ_0 , σ_ξ^2 , $\tilde{\tau}$, and ν_0 . In addition, the bandwidth of $|\bar{A}(\nu)|^2$ (centered at $\nu = \nu_0$) and $|\overline{|A|^2}(\nu)|^2$ (centered at $\nu = 0$) will simply be assumed to be much larger than f_{rep} . For high-quality active mode locking, we expect $\Lambda_0 \ll \sigma_\xi^2$ and $\sqrt{\Lambda_0} \ll \tilde{\tau}^{-1}$ but $\sigma_\xi \ll \tilde{\tau}$. We choose $\tilde{\tau} = 40f_{\text{rep}}^{-1}$, $\sigma_\xi = 5 \times 10^{-3}f_{\text{rep}}^{-1}$, and $\Lambda_0 = 2.5 \times 10^{-9}f_{\text{rep}}^{-1}$ with $f_{\text{rep}} = 1$.

In Fig. 1 are shown $S_f^{(1)}(\nu)$ (solid) and the envelope $\exp(-4\pi^2\nu^2\sigma_\xi^2)$ of $S_f^{(0)}(\nu)$ (dashed). $S_f^{(1)}(\nu)$ dominates the behavior of the comb-line pedestals (see Figs. 2 and 4 below), while $\exp(-4\pi^2\nu^2\sigma_\xi^2)$ sets the scale of the spectral weight of the narrow comb-line central peaks. The latter may be misleading, as the low-order peaks in $S_f^{(0)}(\nu)$ may be of far higher magnitude than the scale suggests, as can be seen in Fig. 2, which shows the contributions $S_{f,\text{max}}^{(0)}(\nu)$ and $S_{f,\text{max}}^{(1)}(\nu)$ to the comb-line maxima $S_{f,\text{max}}(\nu) = S_{f,\text{max}}^{(0)}(\nu) + S_{f,\text{max}}^{(1)}(\nu)$ obtained by setting the complex exponential in Eq. (21) to 1, where

$$S_{f,\text{max}}^{(0)}(\nu) = e^{-4\pi^2\nu^2\sigma_\xi^2} \frac{1 - e^{-8\pi^2\nu^2\Lambda_0}}{1 + e^{-8\pi^2\nu^2\Lambda_0} - 2e^{-4\pi^2\nu^2\Lambda_0}}, \quad (24)$$

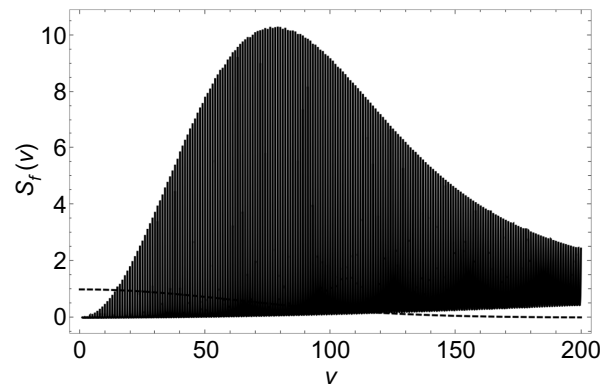


FIG. 1. The contributions $S_f^{(0)}(\nu)$ and $S_f^{(1)}(\nu)$ to $S_f(\nu)$ for $\sigma_\xi = 0.0025$, $\tilde{\tau} = 20$, and $\Lambda_0 = 2.5 \times 10^{-9}$. The frequency ν is in units of f_{rep} . The dashed curve is the envelope $\exp(-4\pi^2\nu^2\sigma_\xi^2)$ of $S_f^{(0)}(\nu)$; the solid curve is $S_f^{(1)}(\nu)$.

$$\begin{aligned}
S_{f,\text{max}}^{(1)}(\nu) &= e^{-4\pi^2\nu^2\sigma_\xi^2} \sum_{k=-\infty}^{\infty} \left[\exp\left(4\pi^2\nu^2\sigma_\xi^2 e^{-2|k|/\tilde{\tau}}\right) - 1 \right] \\
&\times e^{-4\pi^2\nu^2\Lambda_0|k|}. \quad (25)
\end{aligned}$$

$S_{f,\text{max}}^{(0)}(\nu)$ (solid) and $S_{f,\text{max}}^{(1)}(\nu)$ are plotted on a logarithmic scale to display functions with large dynamic range. This figure illustrates the dominance of $S_f^{(0)}(\nu)$ over $S_f^{(1)}(\nu)$ for orders $n \lesssim 150$ for the chosen parameters and of $S_f^{(1)}(\nu)$ over $S_f^{(0)}(\nu)$ for orders $n \gtrsim 150$ in determining the overall comb-line height. In addition, one notes that the comb lines broaden with increasing n . The comb line at zero frequency $\nu = 0$ ($n = 0$) is a pure Dirac δ function and no pedestal is present. Clearly, timing jitter can have no impact on the dc component of $S_f(\nu)$. Note that the bandwidth of

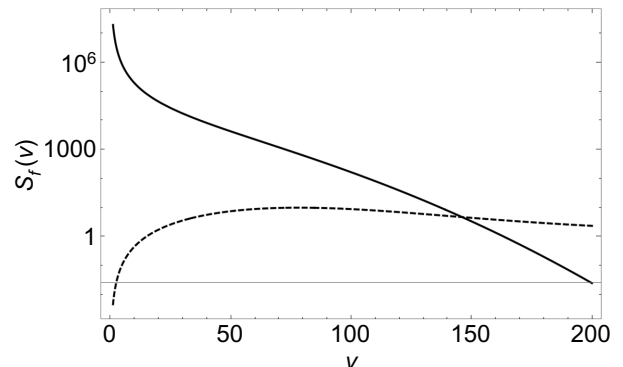


FIG. 2. $S_{f,\text{max}}^{(0)}(\nu)$ (solid) [maxima of $S_f^{(0)}(\nu)$] and $S_{f,\text{max}}^{(1)}(\nu)$, (dashed) [maxima of $S_f^{(1)}(\nu)$] on a logarithmic scale for $\sigma_\xi = 0.0025$, $\tilde{\tau} = 20$, and $\Lambda_0 = 2.5 \times 10^{-9}$. The frequency ν is in units of f_{rep} .

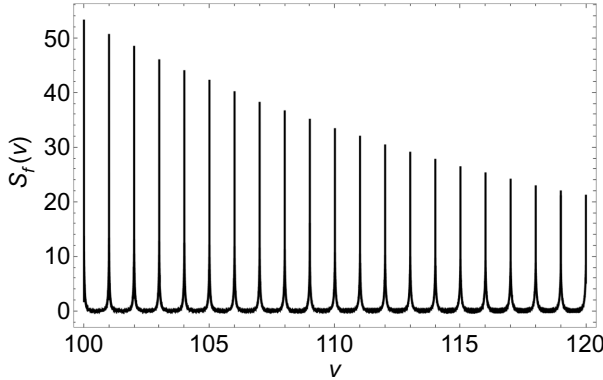


FIG. 3. $S_f(v)$ for $\sigma_\xi = 0.0025$, $\tilde{\tau} = 20$, and $\Lambda_0 = 2.5 \times 10^{-9}$ for comb orders $n \in [100, 120]$. The frequency v is in units of f_{rep} .

$S_f(v)$ —even in the absence of accounting for the power spectrum of the pulse envelope for the OFC or for the MFC (not included in the figure)—is limited by the timing jitter itself. The reduction in peak height and concurrent broadening with increasing n are both connected to the phase noise for comb line n given the timing fluctuation $\xi(t)$. Setting aside the effect of Λ_0 , the standard deviation σ_ϕ of the phase noise for comb line n scales as $\sigma_\phi = 2\pi n f_{\text{rep}} \sigma_\xi$.

MFCs will be dominated by $S_f^{(0)}(v)$ and involve low orders $n \sim 1$. The MFC PSD is $S_f(v) = \overline{|\mathcal{A}|^2(v)}^2 S_f(v)$, whence the MFC is obtained by multiplying $S_f(v)$ by $\overline{|\mathcal{A}|^2(v)}^2$. Depending on the bandwidth of $\overline{|\mathcal{A}|^2(v)}^2$, the MFC bandwidth will be dominated by $\overline{|\mathcal{A}|^2(v)}^2$ or $S_f^{(0)}(v)$,

or in the intermediate case will involve both. OFCs, however, are centered around v_0 . The relevant comb orders n may be as low as tens in mid-IR lasers [50] ranging to approximately 10^8 in standard Ti:sapphire lasers. The OFC is $S_E(v) = |\bar{\mathcal{A}}(v)|^2 S_f(v)$. Therefore, the OFC is obtained by multiplying $S_f(v)$ by $|\bar{\mathcal{A}}(v)|^2$. Depending on the parameters, both $S_f^{(0)}(v)$ and $S_f^{(1)}(v)$ or only $S_f^{(1)}(v)$ may contribute significantly to $S_E(v)$. As an example, consider $S_f(v)$ for $n \in [100, 120]$ for the parameters above in Fig. 3. In this case, the contribution from $S_f^{(0)}(v)$ is responsible for the narrow central peak of each comb line, which is Lorentzian in shape, while $S_f^{(1)}(v)$ dominates the pedestals. In addition, the pedestals from neighboring comb lines begin to merge, giving rise to a so-called underlying continuum.

Figure 4 shows details of the comb lines for $n = 1$, 100, 150, and 200 on logarithmic scales. The nature of the comb line shape is evident here, with a narrow central Lorentzian peak atop a broader pedestal. As n increases, the contribution of the pedestal and underlying continuum increasingly obscures the central peak. Referring to Fig. 2, the crossover between orders with peak height dominated by $S_f^{(0)}(v)$ (Lorentzians) to $S_f^{(1)}(v)$ (pedestals) occurs near $n = 150$ for the parameters used for these figures.

Before we conclude this section, we briefly discuss the acf $F(\tau) = \langle f(t)f(t-\tau) \rangle$ of the signal $f(t)$. In the sequel, we neglect the effect of timing jitter in the locking oscillator, as the time scale Λ_0^{-1} is typically much longer than $\tilde{\tau}$. $F(\tau)$ is the inverse Fourier transform of $S_f(v)$. Rather than attempt the inverse Fourier transform of the results for

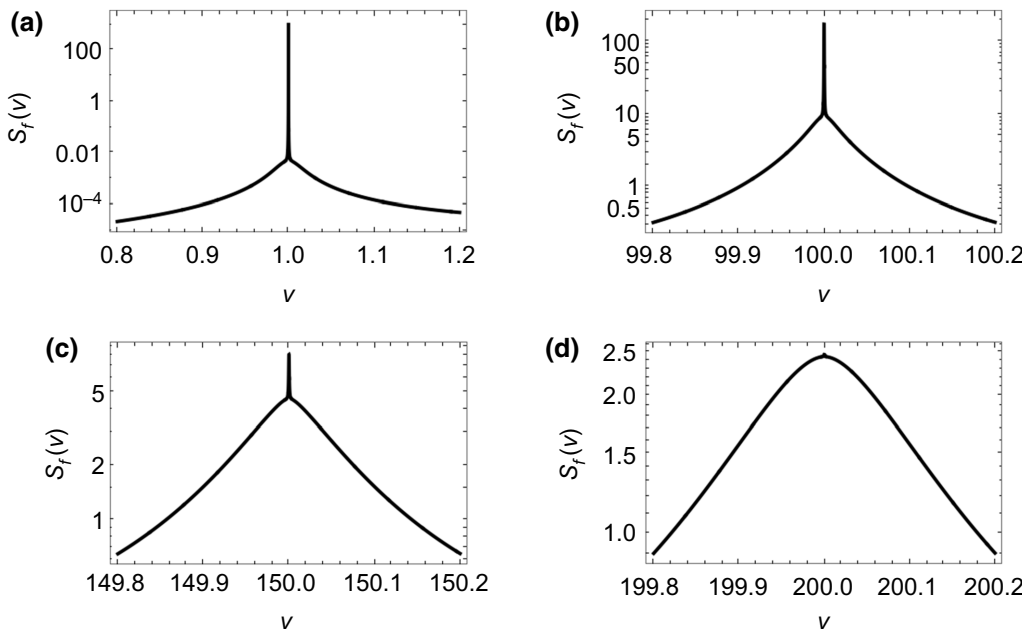


FIG. 4. The order (a) $n = 1$, (b) 100, (c) 150, and (d) 200 line shape of $S_f(v)$ on a logarithmic scale for $\sigma_\xi = 0.0025$, $\tilde{\tau} = 20$, and $\Lambda_0 = 2.5 \times 10^{-9}$. The frequency v is in units of f_{rep} .

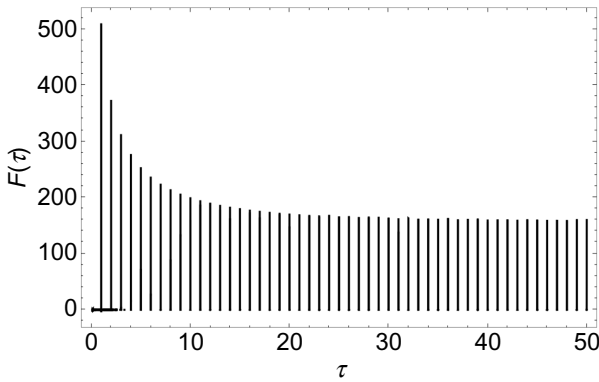


FIG. 5. A plot of the acf $F(\tau)$ for $\sigma_\xi = 0.0025$, $\tilde{\tau} = 20$, and $\Lambda_0 = 0$. The time τ is in units of f_{rep}^{-1} .

$S_f(\nu)$ above, we turn to $f(t)$ in the form of Eq. (10). We have

$$\begin{aligned} F(\tau) &= \langle \delta[t - \xi_{k_1} - k_1 t_{\text{rep}}] \delta[t - \tau - \xi_{k_2} - k_2 t_{\text{rep}}] \rangle \\ &= \sum_{k=-\infty}^{\infty} \langle \delta[\tau - \Xi_{k,0} - kt_{\text{rep}}] \rangle \\ &= \langle v_{\text{rep}} \text{III}[\tau - \Xi(\tau, 0)] \rangle = \sum_{k=-\infty}^{\infty} e^{2\pi i k \tau} \langle e^{2\pi i k \Xi(\tau, 0)} \rangle. \end{aligned} \quad (26)$$

$\Xi(t_1, t_2) = \xi(t_1) - \xi(t_2)$, where $\xi(kt_{\text{rep}}) = \xi_k$, and $\xi(t)$ obeys the same continuous random process from which ξ_k is obtained. We also assume that $\tau_\xi \ll t_{\text{rep}}$. Thus

$$\begin{aligned} F(\tau) &= \sum_{k=-\infty}^{\infty} e^{2\pi i k \tau} e^{-2\pi^2 k^2 \sigma_\Xi^2(\tau)} \\ &= \frac{1}{\sqrt{2\pi \sigma_\Xi^2(\tau)}} \exp\left[-\frac{\tau^2}{2\sigma_\Xi^2(\tau)}\right] \vartheta_3 \\ &\times \left(-\frac{i\tau}{2\sigma_\Xi^2(\tau)}, \exp\left[-\frac{1}{2\sigma_\Xi^2(\tau)}\right]\right) \end{aligned} \quad (27)$$

where $k = k_1 - k_2$ and $\vartheta_3(u, q)$ is an elliptic theta function, $\vartheta_3(u, q) = 1 + 2 \sum_{n=1}^{\infty} q^{n^2} \cos 2nu$. Although the last expression in terms of the elliptic theta function is compact, we do not find it to be very useful for numerical computations in our parameter range.

In Fig. 5, we plot $F(\tau)$ for $\sigma_\xi = 0.0025$, $\tilde{\tau} = 20$, and $\Lambda_0 = 0$. We see an enhanced acf for $\tau \lesssim \tilde{\tau}$. The peaks are of duration determined by σ_ξ . At later times, the acf remains strong—which is not surprising, since σ_ξ is small. In other words, apart from the timing jitter, the locked oscillator has absolute timing imposed (here assuming $\Lambda_0 = 0$) on it by the locking oscillator.

VI. CONCLUSION

We consider PSD $S_f(\nu)$ and acf function $F(\tau)$ for an otherwise periodic impulse train subject to timing jitter and relate $S_f(\nu)$ to the PSDs $S_E(\nu)$ and $S_I(\nu)$ of OFCs and MFCs, respectively.

$S_f(\nu)$ is shown to consist of two contributions: a non-periodic comb of narrow Lorentzian peaks $S_f^{(0)}(\nu)$ and a set of pedestals $S_f^{(1)}(\nu)$. For low comb-line order n , $S_f^{(0)}(\nu)$ dominates; however, at a crossover value of n related to the parameters chosen, eventually $S_f^{(1)}(\nu)$ dominates. In the case of an ideal locking oscillator ($\Lambda_0 = 0$), $S_f^{(0)}(\nu)$ is a Dirac comb modulated by a broad frequency envelope falling off at large ν . In the large- n limit, the pedestals wash out to provide a uniform background of unit height with an increasingly weak sinusoidal modulation. We also show that for practical OFCs, the high-frequency limit is not attained, as is evidenced by the observation of OFC lines.

$S_E(\nu)$ and $S_I(\nu)$ are given by the expressions of Eqs. (2) and (3). Thus, the comb line shapes themselves are given by $S_f(\nu)$ with an additional filter imposed by the single-pulse envelope. Note that we find a strong tendency for MFC lines to be narrower than OFC lines. This is a consequence, first, of the fact that for a given timing jitter $\xi(t)$, the phase-noise standard deviation for a comb line of order n scales with the frequency as $\sigma_{\phi,n} = 2\pi n \sigma_\xi$. In addition, for small n , as is relevant to MFCs, the pedestals play a relatively smaller role than for intermediate n relevant to OFCs. We also note that the observation of a narrow central comb line lying atop a broader pedestal has been seen many times (see, e.g., Refs. [24,25]), in agreement with our predictions; our tractable treatment makes clear the origin of this effect.

With regard to $F(\tau)$, the acf of $f(t)$ is a sequence of peaks with an enhanced acf within $\tau \lesssim \tilde{\tau}$, centered at times indicated by the period of the original signal in the absence of timing jitter. The widths of the acf peaks are determined largely by σ_ξ .

To conclude, we present a model for the effect of timing jitter on the PSD $S_f(t)$ of the signal $f(t)$ consisting of an ideal periodic impulse train, i.e., in the absence of the timing jitter. From $S_f(\nu)$, we obtain $S_E(\nu)$ and $S_I(\nu)$, the PSDs of the OFC and MFC. Our approach, incorporating aspects of Ref. [4,20], is essentially exact, allowing for a weak approximation appropriate to cases when the jitter is weak ($\sigma_\xi \ll 1$) and slow ($\tilde{\tau} \gg 1$). Our main findings are as follows. (1) The PSDs $S_E(\nu)$ and $S_I(\nu)$ for the OFC and MFC are straightforwardly obtained from $S_f(\nu)$. The OFC and MFC are expressed using a small number of generic empirical parameters. The approach is heuristic and transparent and can be applied to measured OFC and MFC spectra, rather than focusing on the detailed physical mechanisms underlying timing jitter in a specific laser. The calculations are presented as a model to assist in

understanding the nature of timing jitter without reference to any physical mechanism for the jitter, but may also provide a way to model specific physical realizations provided that the system conforms to some degree with our assumptions. We also point out that in a field dominated by consideration of physical mechanisms for noise in specific systems, a more general approach such as presented here has obvious heuristic and pedagogic value. (2) Our treatment brings to the fore the stochastic processes, making clear the key step of replacing the Fokker-Planck equation following from the Adler equation with an additional white-noise term by an OU process. (3) For a given set of laser parameters, the MFC is dominated by comb lines with a narrow line center and a weak and broader pedestal, while the OFC has broader and weaker line centers and broad and stronger pedestals. The MFC lines tend to be narrower than OFC lines for the same MLL.

ACKNOWLEDGEMENTS

We gratefully acknowledge the support of Conseil Régional Grand Est and CPER SusChemProc. We declare no conflicts of interest.

APPENDIX

We consider a continuous random variable $\xi(t)$ that determines the timing jitter $\xi_k = \xi(kt_{\text{rep}})$. $\xi(t)$ is known as a stochastic delay [44]. This is physically reasonable, as ξ_k is determined by fluctuations in the laser-cavity length and refractive index. The timing-jitter model for $\xi(t)$ is provided by Ref. [4]. This work treats timing jitter in a hybrid MLL that combines active and passive mode locking. We begin with Eq. (4.7) of Ref. [4], which describes the timing dynamics. This is the Adler equation [47]. We later assume that the modulation time is equal to the round-trip time in the laser cavity, i.e., both rates are equal to f_{rep} , enabling us to drop the drift term. This maintains $\xi(t)$ near zero (provided that $\sigma_\xi \ll 1$ and mode locking is successful). In terms of our parameters, we can write the Adler equation as

$$2\pi f_{\text{rep}} \dot{\xi} = -2\pi f_{\text{rep}} \varepsilon - \zeta \sin 2\pi f_{\text{rep}} \xi; \quad (\text{A1})$$

ε is proportional to the detuning of the active-locking frequency from the laser-cavity round-trip frequency. We shall later set $\varepsilon = 0$. In order to map the parameters onto those of an actual laser, see Ref. [4]. We shall, however, parametrize the problem later in terms of two empirical parameters, viz., the variance σ_ξ^2 and correlation time $\tilde{\tau}$ of ξ .

In a self-sustaining oscillator ($\zeta = 0$), there is no restoring force to bring any drift in the timing back toward zero, implying that the conditional probability distribution of $\xi(t)$, given an initial value, scales as t [4,20]. For the active MLL, however, the timing jitter experiences a restoring

force. In this case, unlike that of the self-sustaining oscillator, $\xi(t)$ may be considered as a stationary random variable. In essence, as shown in Ref. [4], for $\sigma_\xi \ll 1$, $\xi(t)$ is subject to a harmonic potential $U(\xi) = \frac{1}{2}\zeta\xi^2$ that provides a Hooke's-law restoring force. We will then use the resulting Langevin equation to obtain a Fokker-Planck equation. The case of $\zeta = 0$ corresponds to a Wiener process describing one-dimensional diffusion of $\xi(t)$; for σ_ξ sufficiently small, we can approximate the sinusoid in Eq. (A1) by the leading term in its power-series expansion, resulting in an OU process [45] describing one-dimensional diffusion in a harmonic potential.

If we add a primary white-noise source $v(t)$ to Eq. (A1), the result is the Langevin equation in the strong-friction limit of one-dimensional Brownian motion of the form

$$\gamma \dot{\xi} = F(\xi) + sv(t), \quad (\text{A2})$$

where $-\gamma \dot{\xi}$ is the frictional force, $F(\xi)$ is an external force, and s is the amplitude of the primary white-noise source $v(t)$. To correspond with Eq. (A1), we take

$$F(\xi) = -\varepsilon - \frac{\zeta}{2\pi f_{\text{rep}}} \sin 2\pi f_{\text{rep}} \xi, \quad (\text{A3})$$

leaving the dependence on γ for the present. Shortly, we will take $\varepsilon = 0$, as our interest is in the case where the laser is stably active locked. Of course, all parameters must be tied to the underlying physics of the particular MLL. The corresponding Fokker-Planck equation is

$$\partial_t p(\xi, t | \xi_0, t_0) = \left[\frac{s^2}{2\gamma^2} \partial_\xi^2 - \frac{1}{\gamma} \partial_\xi F(\xi) \right] p(\xi, t | \xi_0, t_0), \quad (\text{A4})$$

where $p(\xi, t | \xi_0, t_0)$ is the conditional probability density of finding the phase at ξ at time t given an initial phase ξ_0 at t_0 . The steady-state solution, i.e., the PDF of ξ , which we denote by g_{σ_ξ} , is proportional to the Boltzmann distribution $\exp[-\beta U(\xi)]$ where $F(\xi) = -\partial_\xi U(\xi)$ [51,52] and $\beta = (k_B T)^{-1}$, where k_B is the Boltzmann constant and T is the temperature.

If the timing jitter satisfies $\sigma_\xi \ll 1$, we can approximate the sinusoid in $F(\xi)$ by its leading term, viz., $F(\xi) = -\varepsilon - \zeta \xi$. [With the sinusoidal term in $F(\xi)$, there will always be phase fluctuations the energy of which exceeds the maximum of the potential. If $\sigma_\xi \ll 1$, this is negligible]. Finally, substituting $F(\xi) = -\varepsilon - \zeta \xi$ and changing to conventional thermodynamic parameters gives

$$\partial_t p(\xi, t | \xi_0, t_0) = D [\partial_\xi^2 + \beta(\varepsilon + \zeta \xi)] p(\xi, t | \xi_0, t_0), \quad (\text{A5})$$

where ζ is seen to be the spring constant of Hooke's law, $D = s^2/2\gamma^2$, and $\beta = 2\zeta/s^2$. Henceforth, we set $\varepsilon = 0$. This is the Fokker-Planck equation for an OU process [45].

For us, we merely require the steady-state probability distribution

$$g_{\sigma_\xi}(\xi) = p(\xi, \infty | \xi_0, t_0) = \frac{1}{\sqrt{2\pi\sigma_\xi^2}} e^{-(\xi^2/2\sigma_\xi^2)} \quad (\text{A6})$$

and the structure factor $\sigma_\Xi^2(\tau) = \langle \Xi^2(\tau, 0) \rangle$, which can be expressed in terms of $\sigma_\xi^2(\tau) = \langle \xi(\tau)\xi(0) \rangle$ as

$$\begin{aligned} \sigma_\Xi^2(\tau) &= \langle \Xi^2(\tau, 0) \rangle = \langle [\xi(\tau) - \xi(0)]^2 \rangle \\ &= 2[\langle \xi^2(0) \rangle - \langle \xi(\tau)\xi(0) \rangle] \\ &= 2[\sigma_\xi^2 - \sigma_\xi^2(\tau)], \end{aligned} \quad (\text{A7})$$

where $\sigma_\xi^2 = \sigma_\xi^2(0)$ is the variance of $\xi(t)$. Moreover, $\sigma_\xi^2(\tau) = \langle \xi(\tau)\xi(0) \rangle = \sigma_\xi^2 e^{-2|\tau|/\tilde{\tau}}$. This roughly corresponds to Eq. (72) of Ref. [10].

-
- [1] D. K. Kuizenga and A. E. Siegman, FM and AM mode locking of the homogeneous laser—Part I: Theory, *IEEE J. Quantum Electron.* **QE-6**, 694 (1970).
 - [2] A. J. Maria, D. A. Stetser, and H. Heyneau, Self-mode locking with saturable absorbers, *Appl. Phys. Lett.* **8**, 174 (1966).
 - [3] L. E. Hargrove, R. L. Fork, and M. A. Pollack, Locking of He-Ne laser modes induced by synchronous intracavity modulation, *Appl. Phys. Lett.* **5**, 4 (1964).
 - [4] H. A. Haus and H. L. Dyckman, Timing of laser pulses produced by combined passive and active mode-locking, *Int. J. Electronics* **44**, 225 (1978).
 - [5] F. Quinlan, S. Gee, S. Ozharar, and P. J. Delfyett, Ultralow-jitter and -amplitude-noise semiconductor-based mode-locked laser, *Opt. Lett.* **31**, 2870 (2006).
 - [6] H. A. Haus, A theory of forced mode locking, *IEEE J. Quantum Electron.* **QE-11**, 323 (1975).
 - [7] H. A. Haus, Theory of mode locking with a fast saturable absorber, *J. Appl. Phys.* **46**, 3049 (1975).
 - [8] For a recent work accounting for coherent effect, see A. M. Perego, B. Garbin, F. Gustave, S. Barland, F. Prati, and G. J. de Valcárcel, Coherent master equation for laser modelocking, *Nat. Commun.* **11**, 311 (2020).
 - [9] H. A. Haus and P.-T. Ho, Effect of noise on active mode locking of a diode laser, *IEEE J. Quantum Electron.* **QE-15**, 1258 (1979).
 - [10] H. A. Haus and A. Meccozzi, Noise of mode-locked lasers, *IEEE J. Quantum Electron.* **29**, 983 (1993).
 - [11] Y. Takushima, H. Sotobayashi, M. E. Grein, E. P. Ippen, and H. A. Haus, in *Proc. SPIE 5595, Active and Passive Optical Components for WDM Communications IV* (SPIE, Philadelphia, Pennsylvania, 2004).
 - [12] D. R. Hjelme and A. R. Mickelson, Theory of timing jitter in actively mode-locked lasers, *IEEE J. Quantum Electron.* **28**, 1594 (1992). The theoretical approach employed here is frequency-based, but is essentially the same as time-domain approaches such as those based on the Haus master equation.
 - [13] J. Kluge, D. Wiechert, and D. von der Linde, Fluctuations in synchronously mode-locked lasers, *Opt. Commun.* **51**, 271 (1984).
 - [14] D. Kühlke, U. Herpers, and D. von de Linde, Characteristics of a hybridly mode-locked laser, *Appl. Phys. B* **39**, 233 (1985).
 - [15] A. D. von der Linde, Characterization of the noise in continuously operating mode-locked lasers, *Appl. Phys. B* **39**, 201 (1986).
 - [16] B. H. Kolner and D. M. Bloom, Electrooptic sampling in GaAs integrated circuits, *IEEE J. Quantum Electron.* **QE-22**, 79 (1986).
 - [17] A. J. Taylor, J. M. Weisenfeld, G. Eisenstein, and R. S. Tucker, Timing jitter in mode-locked and gain-switched InGaAsP injection lasers, *Appl. Phys. Lett.* **49**, 681 (1986).
 - [18] J. E. Bowers, P. A. Morton, A. Mar, and S. W. Corzine, Actively mode-locked semiconductor laser, *IEEE J. Quantum Electron.* **25**, 1426 (1989).
 - [19] D. Burns, A. Finch, W. Sleat, and W. Sibbett, Noise characterization of a mode-locked InGaAsP semiconductor diode laser, *IEEE J. Quantum Electron.* **26**, 1860 (1990).
 - [20] M. Lax, Classical noise. V. Noise in self-sustained oscillators, *Phys. Rev.* **160**, 290 (1967).
 - [21] S. A. Diddams, K. Vahala, and T. Udem, Optical frequency combs: Coherently uniting the electromagnetic spectrum, *Science* **369**, 267 (2020).
 - [22] N. Picqué and T. W. Hänsch, Frequency comb spectroscopy, *Nat. Photon.* **13**, 146 (2019).
 - [23] T. Fortier and E. Baumann, 20 years of developments in optical frequency comb technology and applications, *Commun. Phys.* **2**, 153 (2019).
 - [24] S.-C. Chan, G.-Q. Xia, and J.-M. Liu, Optical generation of a precise microwave frequency comb by harmonic frequency locking, *Opt. Lett.* **32**, 1917 (2007).
 - [25] Y.-S. Juan and F.-Y. Lin, Microwave-frequency-comb generation utilizing a semiconductor laser subject to optical injection from an optoelectronic feedback laser, *Opt. Lett.* **34**, 1636 (2009).
 - [26] J. Yao, Microwave photonics, *J. Lightwave Technol.* **27**, 314 (2009).
 - [27] D. Marpaung, J. Yao, and J. Capmany, Integrated microwave photonics, *Nat. Photon.* **13**, 80 (2019).
 - [28] A. B. Matsko and L. Maleki, On timing jitter of mode locked Kerr frequency combs, *Opt. Express* **21**, 28862 (2013).
 - [29] D. Kwon, C. G. Jeon, J. Shin, M. S. Heo, S. E. Park, Y. Song, and J. Kim, Reference-free, high-resolution measurement method of timing jitter spectra of optical frequency combs, *Sci. Rep.* **7**, 40917 (2016).
 - [30] M. Ablowitz, B. Ilan, and S. T. Cundiff, Noise-induced linewidth in frequency combs, *Opt. Lett.* **31**, 1875 (2006).
 - [31] J. K. Wahlstrand, J. T. Willits, C. R. Menyuk, and S. T. Cundiff, The quantum-limited comb lineshape of a mode-locked laser: Fundamental limits on frequency uncertainty, *Opt. Express* **16**, 18624 (2008).
 - [32] M. Kourogi, K. Nakagawa, and M. Ohtsu, Wide-span optical frequency comb generator for accurate optical frequency difference measurement, *IEEE J. Quantum Electron.* **29**, 2693 (1993).

- [33] J. Ye, L. S. Ma, T. Day, and J. L. Hall, Highly selective terahertz optical frequency comb generator, *Opt. Lett.* **22**, 301 (1997).
- [34] P. J. Delfyett, I. Ozdur, N. Hoghooghi, M. Akbulut, J. Davila-Rodriguez, and S. Bhooplapur, Advanced ultrafast technologies based on optical frequency combs, *IEEE J. Sel. Top. Quantum Electron.* **18**, 258 (2012).
- [35] A. K. Wójcik, P. Malara, R. Blanchard, T. S. Mansuripur, F. Capasso, and A. Belyanin, Generation of picosecond pulses and frequency combs in actively mode locked external ring cavity quantum cascade lasers, *Appl. Phys. Lett.* **103**, 231102 (2013).
- [36] D. Burghoff, T.-Y. Kao, N. Han, C. W. I. Chan, X. Cai, Y. Yang, D. J. Hayton, J.-R. Gao, J. L. Reno, and Q. Hu, Terahertz laser frequency combs, *Nat. Photon.* **8**, 462 (2014).
- [37] V. Panapakkam, A. P. Anthur, V. Vujicic, R. Zhou, Q. Gaimard, K. Merghem, G. Aubin, F. Lelarge, E. A. Viktorov, L. P. Barry, and A. Ramdane, Amplitude and phase noise of frequency combs generated by single-section InAs/InP quantum-dash-based passively and actively mode-locked lasers, *IEEE J. Quantum Electron.* **52**, 1300207 (2016).
- [38] D. S. Citrin, Carrier-envelope-stabilized optical frequency combs: Effect of fluctuations on the comb line shape, *J. Opt. Soc. Am. B* **38**, 719 (2021).
- [39] D. S. Citrin, Unified theory of the power spectral density of injection-locked optoelectronic oscillators, *J. Lightwave Technol.* submitted.
- [40] J. H. Eberly and K. Wódkiewicz, The time-dependent physical spectrum of light, *J. Opt. Soc. Amer.* **67**, 1252 (1977).
- [41] N. Wiener, Generalized harmonic analysis, *Acta Math.* **55**, 117 (1930).
- [42] A. Khintchine, Korrelationstheorie der stationären stochastischen Prozesse, *Math. Ann.* **109**, 604 (1934).
- [43] IEEE Standard Definitions of Physical Quantities for Fundamental Frequency and Time Metrology: Random Instabilities, IEEE Std 1139–1999.
- [44] O. A. Z. Leneman, Random sampling of random processes: Optimum linear interpolation, *J. Franklin Inst.* **281**, 302 (1966).
- [45] G. E. Uhlenbeck and L. S. Ornstein, On the theory of Brownian motion, *Phys. Rev.* **36**, 823 (1930).
- [46] I. Florescu, *Probability and Stochastic Processes* (Wiley, Hoboken, New Jersey, 2014).
- [47] See Eq. (9c) of R. Adler, A study of locking phenomena in oscillators, *Proc. IRE* **43**, 351 (1946).
- [48] G. B. Rybicki, Notes on Gaussian Random Functions with Exponential Correlation Functions (Ornstein-Uhlenbeck Process), unpublished. Available at https://www.lanl.gov/DLDSTP/fast/OU_process.pdf.
- [49] A. V. Balakrishnan, On the problem of time jitter in sampling, *IRE Trans. Inf. Theory* **8**, 226 (1962).
- [50] J. Hillbrand, N. Opacak, M. Piccardo, H. Schneider, G. Strasser, F. Capasso, and B. Schwarz, Mode-locked short pulses from an 8 μ m wavelength semiconductor laser, *Nat. Commun.* **11**, 5788 (2020).
- [51] W. Dieterich, I. Peschel, and W. R. Schneider, Diffusion in periodic potentials, *Z. Phys. B* **27**, 177 (1977).
- [52] A. K. Das and P. Schwendimann, Fokker-Planck equation for a periodic potential, *Physica* **89A**, 605 (1977); A. K. Das, Stochastic diffusion in a periodic potential, *Physica* **98A**, 528 (1979).